JOURNAL OF FOOD AND DRUG ANALYSIS 25 (2017) 654–666

Available online at www.sciencedirect.com

ScienceDirect

journal homepage: www.jfda-online.com

Original Article

Microencapsulation of fish oil using supercritical antisolvent process

Fahim Tamzeedul Karim [a], *Kashif Ghafoor* [b], *Sahena Ferdosh* [c], *Fahad Al-Juhaimi* [b], *Eaqub Ali* [d], *Kamaruzzaman Bin Yunus* [c], *Mir Hoseini Hamed* [e], *Ashraful Islam* [f], *Mohammad Asif* [g], *Mohammed Zaidul Islam Sarker* [a,*]

[a] *Faculty of Pharmacy, International Islamic University Malaysia, Kuantan Campus, 25200 Kuantan, Pahang, Malaysia*
[b] *Department of Food Science and Nutrition, King Saud University, Riyadh 11451, Saudi Arabia*
[c] *Faculty of Science, International Islamic University Malaysia (IIUM), Kuantan Campus, 25200 Kuantan, Pahang, Malaysia*
[d] *Nanotechnology and Catalysis Research Centre (NanoCat), University of Malaya, Kuala Lumpur 50603, Malaysia*
[e] *Faculty of Food Science and Technology, Universiti Putra Malaysia, 43400 Serdang, Selangor DE, Malaysia*
[f] *Department of Pharmacy, University of Asia Pacific, Dhanmondi, Dhaka, Bangladesh*
[g] *Department of Chemical Engineering, King Saud University, Riyadh 11421, Saudi Arabia*

ARTICLE INFO

Article history:
Received 4 August 2016
Received in revised form
21 November 2016
Accepted 24 November 2016
Available online 14 February 2017

Keywords:
HPMC
microencapsulation
omega 3
supercritical antisolvent

ABSTRACT

In order to improve the encapsulation process, a newly supercritical antisolvent process was developed to encapsulate fish oil using hydroxypropyl methyl cellulose as a polymer. Three factors, namely, temperature, pressure, and feed emulsion rate were optimized using response surface methodology. The suitability of the model for predicting the optimum response value was evaluated at the conditions of temperature at 60°C, pressure at 150 bar, and feed rate at 1.36 mL/min. At the optimum conditions, particle size of 58.35 μm was obtained. The surface morphology of the micronized fish oil was also evaluated using field emission scanning electron microscopy where it showed that particles formed spherical structures with no internal voids. Moreover, *in vitro* release of oil showed that there are significant differences of release percentage of oil between the formulations and the results proved that there was a significant decrease in the *in vitro* release of oil from the powder when the polymer concentration was high.

* *Corresponding author*. Department of Pharmaceutical Technology, Faculty of Pharmacy, International Islamic University Malaysia, Kuantan Campus, 25200 Kuantan, Pahang, Malaysia.
E-mail address: zaidul@iium.edu.my (M.Z.I. Sarker).
http://dx.doi.org/10.1016/j.jfda.2016.11.017

1. Introduction

Fish oil is considered a good source of omega-3 and omega-6 polyunsaturated fatty acids (PUFAs) including eicosapentaenoic acid (EPA) and docosahexaenoic acid (DHA) which have been shown to reduce the risk of coronary heart disease, hypertension, thrombosis, inflammations, rheumatoid arthritis, symptoms of allergies (atopic eczema), some types of cancer, and the rate of ageing, and promote the development and functions of central nervous system, thereby helping cell signaling and gene expression [1–3]. The common and widely researched ω3 PUFAs are EPA (5 double bonds) and DHA (6 double bonds).

Microencapsulation is defined as the technique where solid, liquid, and gaseous materials are enclosed in small capsules or microcapsules that release their content at a controlled rate over prolonged periods of time [4]. In this technique, the core material is embedded in a protective layer of different composition and ratio of polymer. Here, the liquid is transformed into a powder by different microencapsulation techniques and the powder has better stability against light and oxidative degradation, and is easier to incorporate into a variety of food matrices. The supercritical antisolvent technique has a great potential in particle engineering as carbon dioxide (CO_2) is nontoxic, nonflammable, nonpolluting, and relatively cheap. Its critical state of pressure ($P_c = 7.3$ MPa) and temperature ($T_c = 31.1^{\circ}C$) are readily accessible in practical applications. Supercritical antisolvent processes are based on solution of the solutes into the conventional liquid solvent using supercritical fluid. The supercritical CO_2 saturates the liquid solvent resulting in the precipitation of solute by an antisolvent effect [5] (Figure 1). The advantages of supercritical antisolvent processes include the control of the particle morphology on a very wide range from nanoparticles to microparticles. Supercritical antisolvent is amenable to continuous processing which is very important for large-scale production of microsized and nanosized particles. Freshly precipitated particles can easily be collected from the high pressure vessel and the supercritical fluid where organic solvents can be drained continuously from the system. The disadvantages of these processes are the longer washing period due to agglomeration and aggregation of the particles in the nozzle [5].

A critical step in the production of microcapsules is the selection of appropriate encapsulating material. The selection of encapsulating material can be made from a large variety of natural or synthetic polymers depending on the stability and release characteristics anticipated from the final microcapsule. It has been reported that the composition as well as the physical and chemical properties of the shell material can influence the functionality of the final microcapsule and the processing technologies to be used for microencapsulation [6]. According to Augustin and Sanguansri [7], a good encapsulating material should have neutral taste and odor, low viscosity, good film forming, gelling, and barrier properties. It also can preserve the core from degradation during processing and storage and mask any unpleasant taste or odor related with the bioactive core when added into foods.

Oils containing PUFAs can be encapsulated in a variety of polymers including modified starches, glucose, trehalose, maltodextrins, hydroxypropyl methyl cellulose (HPMC), lecithin, chitosan, corn syrup solids, gum Arabic, pullulan, whey protein, sodium caseinate, gelatin, alginate, and glycated proteins [8–11]. The two mostly studied wall materials, namely whey protein and maltodextrin, are extensively used for encapsulation of PUFA rich oils. Mehrad et al [12] studied the encapsulation of fish oil by using different combinations of maltodextrin, fish gelatin, and κ carrageenan where a combination of maltodextrin and fish gelatin showed best encapsulation efficiency with high emulsion stability. In another study conducted by Pourashouri et al [13] on encapsulation of fish oil, the authors found that the encapsulating material fish gelatin provided the highest preserving effect on the covering fish oil. Klaypradit and Huang [14] encapsulated tuna oil in whey protein combined with chitosan and maltodextrin by ultrasonic atomization. The materials and process produced microcapsules with good encapsulation efficiency (~80%) and with little loss of DHA and EPA following processing; however, long term stability was not evaluated. HPMC has also been used as a good encapsulating material. Kolanowski et al [15] studied the encapsulation of fish oil using HPMC and methyl cellulose by spray drying where the authors indicated that these carrier materials improved the stability and concentration of fish oil in the powder. Another study was performed by Christensen et al [16] for the encapsulation of fractionated coconut oil with different types of HPMC, where the low viscosity HPMC was found to be a useful solid carrier and the dry emulsions remained physically stable for at least 6 months. Wu and Xiao [17] conducted a study for the encapsulation of fish oil using HPMC and maltodextrin as a carrier material by simple coacervation. It was observed that the oxidative stability of encapsulated fish oil was improved via simple coacervation of HPMC with the best result in the case of replacing malt dextrin by 40% with acacia. Karim et al [18] studied the encapsulation of fish oil using different ratios and mixtures of HPMC 15 cps and HPMC 5 cps where the stability and encapsulation efficiency of fish oil powder was improved when compared to raw fish oil.

At present, there is no published research on the micronization of fish oil using the supercritical antisolvent process. Therefore, the purpose of this study was to investigate the encapsulation of fish oil using HPMC as a carrier material in the supercritical antisolvent process based on supercritical CO_2. The experimental parameters such as temperature (°C), pressure (bar) and feed flow rate (mL/min) were also studied. Additionally, micronized fish oil was also observed under field emission scanning electron microscopy (FESEM).

2. Materials and methods

2.1. *Materials*

HPMC (Methocel E15 Premium LV) was kindly gifted by Incepta Pharmaceuticals Ltd, Dhaka, Bangladesh. Fish oil (20–30% omega-3) was obtained from Sigma-Aldrich Inc. (St Louis, MO, USA). Pepsin derived from porcine mucosa and pancreatin from porcine pancreas (meeting the requirements of US

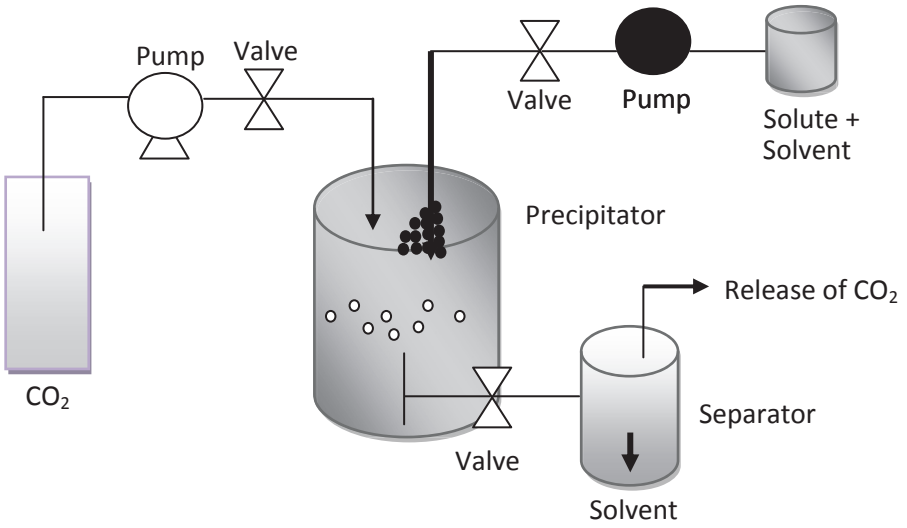

Figure 1 – Schematic diagram of supercritical antisolvent (SAS) process (adapted from Ref. [5]).

Pharmacopeia) were obtained from Sigma-Aldrich Inc. All the other reagents used were of analytical grade. Polyethylene glycol 6000 (PEG 6000) was used as a plasticizer. All the ingredients and polymers used in this study were of food grade.

2.2. Methods

2.2.1. Preparation of microencapsulated fish oil

In this experiment, the in-house supercritical antisolvent system was designed and fabricated according to Chong et al [19] (Figure 2). It consisted of supercritical fluid (SCF) delivery, feed delivery, a precipitation vessel with a capacity of 6 L and a particles collector. Here, purified grade of CO_2, 99.98% purity (MOX, Kuala Lumpur, Malaysia) was used as supercritical fluid. The temperature of the system was controlled by a water-bath throughout the experiment. Liquefied CO_2 was delivered to the vessel using a high pressure pump.

The pressure of the whole system was released before collecting the particles. Therefore, in this study an external particles collector (Figure 3) was designed and fixed at the bottom of the precipitation vessel. The size of inlet was designed in order to have turbulence when supercritical CO_2 entered the particles collector so that the particles were evenly distributed on the surface of the membrane filter. An additional needle valve was installed just after the precipitation vessel to maintain the pressure of the precipitation vessel by closing the valve while collecting the particles. Subsequent experiments could be run after placing the new membrane in the particles collector.

2.2.2. Experimental design using response surface methodology

In this study, response surface methodology was used to determine the optimum condition for the factors affecting the stable encapsulated fish oil powder. The effect of the three experimental factors of X_1: temperature; X_2: pressure; X_3: feed flow rate, on the dependent variable or response in particle size were analyzed. The experimental design was generated using MINITAB software version 16 (Minitab Ltd, Coventry,

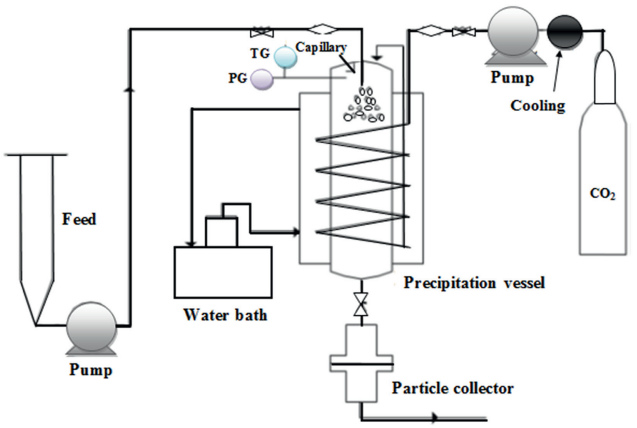

Figure 2 – Schematic diagram of supercritical antisolvent (SAS) system (adapted from Ref. [19]).

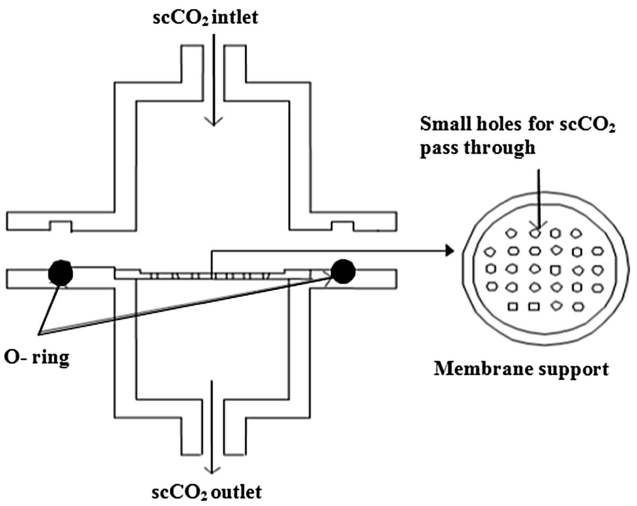

Figure 3 – Particle collector used in supercritical antisolvent (SAS) system (Adapted from Ref. [19]).

United Kingdom). In relation to this, the independent variables are shown in Table 1. Based on Table 1, 15 experimental runs were performed according to Table 2 and the experimental values were fitted according to Eq. (1) as a second-order polynomial equation:

$$y = \beta_0 + \beta_1 X_1 + \beta_2 X_2 + \beta_3 X_3 + \beta_{11} X_1^2 + \beta_{22} X_2^2 + \beta_{33} X_3^2 + \beta_{12} X_1 X_2 + \beta_{13} X_1 X_3 + \beta_{23} X_2 X_3 \quad (1)$$

where, where β_n are constant regression coefficients; y is the response (particle size); X_1: temperature, X_2: pressure, and X_3: feed flow rate.

2.2.3. Characterization of fish oil emulsion

2.2.3.1. Emulsion viscosity. The viscosities of the prepared samples were measured at 20°C with the aid of a viscometer (DV-III Ultra, Brookfield Engineering Laboratories, Inc., Middleboro, USA) fitted with spindle SC4–18 [18]. Samples were placed in the measurement cell of the viscometer and allowed to equilibrate at 20°C. The viscosity measurements for all the samples were carried out with a shear rate ranging from 150 s^{-1} to 300 s^{-1}. Viscosity readings were taken after subjecting the sample to shear for 1 minute. The viscosity was obtained in terms of millipascal-second (mPa.s).

2.2.3.2. Emulsion droplet size. Particle size distribution of the prepared emulsions was measured by laser diffraction using a laser particle size analyzer BT-9300H (Dandong Bettersize Instruments, Dandong, China) and expressed as volume weighted mean, $D_{4,3}$ [18]. Distilled water was used as a dispersant. Each sample was analyzed in triplicate and average data were reported.

2.2.4. Characterization of encapsulated fish oil

2.2.4.1. Moisture content. The moisture content of the spray dried powder was determined using a moisture analyzer (A&D MS-70, A&D Company, Limited, Tokyo, Japan) using the AOAC (2000) method. Initially, about 1 g of powder sample was placed on the heating pan of the moisture analyzer. The moisture evaporates as a result of continuous heating at 105°C and once the mass of the sample achieved a constant value, the experiment stopped automatically.

2.2.4.2. Determination of microencapsulation efficiency. The procedure of determining the total oil content was followed by Anwar and Kunz [20] with some modifications. Firstly, sodium phosphate buffer was prepared by mixing 80 mL solution of monosodium phosphate (5.6 g NaH_2PO_4 in 200 mL distilled water) with 420 mL solution of disodium hydrogen phosphate (14.2 g Na_2HPO_4 in 500 mL distilled water) in a 1 L schott bottle.

Table 1 – Coded and uncoded factors for the design experiments.

Independent variables	Coded factor	Level	
		Low (−1)	High (+1)
Temperature	X_1	40	60
Pressure	X_2	140	160
Feed flow rate	X_3	1	4

Table 2 – Experimental design recommended by MINITAB software version 16.

Run order	Temperature (X_1)	Pressure (X_2)	Feed flow rate (X_3)
1	60	160	2.5
2	60	140	2.5
3	40	150	1.0
4	40	140	2.5
5	50	160	4.0
6	50	150	2.5
7	40	160	2.5
8	40	150	4.0
9	50	150	2.5
10	60	150	1.0
11	50	160	1.0
12	50	140	1.0
13	50	140	4.0
14	50	150	2.5
15	60	150	4.0

Porcine pancreatin (30 mg) was weighed into a clean 50 mL tube where 250 mg of microcapsule powder was added and weighed. Exactly 10 mL sodium phosphate buffer solution was added to this mixture. The vial was vortexed (Vortex Genie 2, Scientific Industries, Bohemia, New York, USA) and placed in an incubator shaker at 37°C at 70 rpm for 1 hour. The tube was then cooled to room temperature and 10 mL ethyl acetate was added to the solution and weighed (W_{sol}). The tube was again vortexed for 3 minutes and centrifuged at 1000 rpm for 10 minutes. Then, approximately 3 mL of organic layer was withdrawn and added to a tared tube and the tube was weighed (W_{ext}). This layer was blanketed under nitrogen gas. The tubes were then uncapped and placed in an oven at 45°C to ensure all the solvents had evaporated, which gave the final weight of the extracted oil (W_{oil}). From this, the amount (g) of total oil extracted from the powder was calculated using Eq. (2):

$$\textit{Total oil}\ (g) = (W_{sol}/W_{ext}) \times W_{oil} \quad (2)$$

The surface oil content of encapsulated powder was determined using extraction with petroleum ether [21]. Spray dried powders (2 g) were weighed and dispersed in 25 mL petroleum ether in a volumetric flask and shaken manually for 8 minutes. Then, the dispersion was filtered through Whatman number 1 filter paper and the collected microparticles were rinsed three times with 15 mL of petroleum ether. The filtrate solution containing the extractable oil was transferred to a tared petri dish to allow solvent evaporation at room temperature. The amount (g) of surface oil on the particles was then calculated from Eq. (3):

$$\textit{Surface oil}\ (g) = \frac{\textit{Amount of extracted oil}}{\textit{Initial mass of the powder particles}} \quad (3)$$

Microencapsulation efficiency (%) was then calculated from the following Eq. (4):

$$\textit{Microencapsulation efficiency}\ (\%) = \frac{\textit{Total oil} - \textit{Surface oil}}{\textit{Total oil}} \quad (4)$$

2.2.4.3. In vitro determination of encapsulated oil after exposure to simulated gastric fluid and simulated intestinal fluid.

The *in vitro* digestion was carried out in two phases; first, the encapsulated oil was exposed to simulated gastric fluid (SGF) containing pepsin and sodium chloride at low pH value [22] and second, an intestinal digestion was simulated by exposing gastric digestion elements to a simulated intestinal fluid (SIF) [23]. The SGF was prepared according to the USP method [24] where 0.64 g of pepsin and 0.4 g of sodium chloride were dissolved in ultrapure water (180 mL). After that hydrochloric acid (1.4 mL, 36% w/v) was added to the solution and the final volume of the solution was made up to 200 mL with ultrapure water. The pH of the solution was ~1.2. The SIF was prepared by dissolving 0.25 g of pancreatin and 1.36 g of potassium dihydrogen phosphate in ultrapure water. Sodium chloride (15.4 mL, 0.2 M) was then added to the solution, which was stirred overnight at 4°C using a magnetic stirrer. The pH of the solution was set to 6.8 with 1 M sodium hydroxide and the final volume of the solution was fixed at 200 mL with ultrapure water.

A 5 g of powder sample was added to 50 mL of SGF in a 250 mL Erlenmeyer flask. The mixture solution was then incubated at 37°C for 2 hours in an incubator shaker (100 rpm) and the pH was set to 6.8 using 1M NaOH. Approximately, 50 mL of SIF was added to the solution and further incubated at the same conditions for another 3 hours. The oil released was extracted three times with 20 mL of petroleum ether. For each extraction, the solvent was added into the sample solution and mixed using a flask shaker for 10 minutes and allowed to stand for 15 min. The extracts were mixed together and the solvent was removed using a rotary evaporator. The oil released from the sample was calculated as a percentage of the total oil in the sample.

2.2.4.4. *Particle size distribution*. The particle size distribution of fish oil powders was measured using laser diffraction particle size analyzer (Malvern 2000 mastersizer, Malvern Instruments Co., Grovewood Road, Malvern, Worcestershire, UK) equipped with an automated dry powder dispersion unit (Scirocco 2000). The particle size distribution was characterized by the volume weighted mean, $D_{4,3}$.

2.2.4.5. *Particle surface morphology*. The morphologies of the powder particles were analyzed through a field emission scanning electron microscope (JEOL JSM-7800F, Japan). The dried powder was mounted on specimen stubs with double-sided adhesive carbon tapes. The specimen was coated with platinum and examined at 1–3 kV with a magnification ranging from 500× to 10,000×.

2.2.4.6. *Bulk density and tapped density of the powder*. Bulk density of microencapsulated powder was determined according to Karim et al [18]. The powder was gently loaded into a 50 mL tared glass cylinder up to 50 mL mark and weighed (W_m). The volume (V_{bulk}) obtained directly from the glass cylinder was used to calculate the bulk density (ρ_{bulk}) based on the following relationship shown in Eq. (5):

$$\rho_{bulk} = W_m / V_{bulk} \tag{5}$$

For tapped density (ρ_{tapped}), approximately 5 g (M) of encapsulated powder was placed into a 50 mL glass cylinder. The powders were repeatedly tapped manually by lifting and dropping the cylinder under its own weight at a vertical distance of 10 cm until negligible difference in volume (V_{tapped}) between succeeding measurements was observed. Then, the tapped density was calculated based on Eq. (6) [25]:

$$\rho_{tapped} = M / V_{tapped} \tag{6}$$

2.2.4.7. *Flowability and cohesiveness of powder*. Flowability and cohesiveness of powder were determined in terms of Carr index (*CI*) and Hausner ratio (*HR*), respectively. Both *CI* and *HR* were calculated from the value of bulk (ρ_{bulk}) using Eq. (7) and tapped (ρ_{tapped}) densities of the powder using Eq. (8):

$$CI = \left(\rho_{tapped} - \rho_{bulk}\right) \Big/ V_{tapped} \times 100 \tag{7}$$

$$HR = \rho_{tapped} \Big/ \rho_{bulk} \tag{8}$$

The scale of flow ability and cohesiveness of the powder particles based on the *CI* and *HR* values are shown in Table 3 [26,27].

2.2.4.8. *Particle density of powder*. Particle density ($\rho_{particle}$) of the powder sample was determined according to A/S Niro Atomizer with some modifications [28]. A powder sample (1 g) was taken in a 10 mL measuring cylinder with a glass stopper. After the addition of 5 mL of petroleum ether, the measuring cylinder was shaken until all the powder particles were suspended. Finally, the rest of the powder particles were rinsed down on the wall of the cylinder by further addition of 1 mL of petroleum ether and the total volume of petroleum ether with suspended powder was recorded. The particle density was calculated using Eq. (9) as shown below:

$$\rho_{particle} = \frac{Powder\ weight}{Total\ volume\ of\ petrolem\ ether\ with\ suspended\ powder - 6} \tag{9}$$

2.2.4.9. *Peroxide value of the powder*. Powder samples were stored in an amber schott bottle at 4°C immediately after spray drying for 28 days. The oxidative stability of microcapsules was monitored in 7 day intervals, and experiments were carried out in triplicate. The peroxide value (PV) was measured to determinate the oxidation process during storage. The PV was determined according to AOCS method of Cd 8-53 with chloroform and glacial acetic acid as solvents [29]. Firstly, approximately 5 g of microencapsulated powder was weighed and added to a 250 mL conical flask with a plastic

Table 3 – Scale of flowability and cohesiveness of powder.

Carr Index (%)	Flow character	Hausner ratio
≤ 10	Excellent	1.00–1.11
11–15	Good	1.12–1.18
16–20	Fair	1.19–1.25
21–25	Passable	1.26–1.34
26–31	Poor	1.35–1.45
32–37	Very poor	1.46–1.59
> 38	Very, very poor	> 1.60

plug and dispersed completely into 12 mL of distilled water by magnetic stirring for 10 minutes. A mixture of 15 mL of chloroform and 30 ml of methanol was added to the solution. After magnetic stirring for 10 minutes, 15 mL of chloroform was added into the mixture and stirred for 2 minutes. Then, 15 mL of distilled water was added and stirred for 5 minutes. The solution was kept still for 30 minutes for the formation of a layer. From the upper layer, 12 mL was pipetted into a weighed and dried 250 mL conical flask and dried at 105°C for 1 hour.

Exactly 12 mL of the chloroform phase, 18 mL of glacial acetic acid, and 1 mL of freshly prepared saturated potassium iodide solution were pipetted into the dried 250 mL conical flask. After shaking it by hand for 10 seconds, the conical flask was placed with a cover in the dark for 3 minutes and then, 30 mL of distilled water and 5 mL of 1% starch solution were added. The mixed solution was titrated under constant agitation with 0.0025N sodium thiosulfate until the blue color disappeared completely. The PV was calculated at mol/kg from Eq. (10):

$$PV = \frac{[((S-B)\times N\times 1000)]}{W} \quad (10)$$

where S is the titration of the sample (in mL), B is the titration of blank (in mL), N is the normality of the sodium thiosulfate solution, and W is the weight of the sample (in g).

3. Results and discussion

3.1. Fitting the response surface models

As shown in Table 4, the lowest actual and predicted responses were 26.490 μm and 25.970 μm, respectively, where the temperature was 60°C, pressure was 160 bar, and the feed flow rate was 2.5 mL/min. The highest actual and predicted responses were 90.930 μm and 88.855 μm, respectively, under prearranged factors which were temperature of 60°C, pressure of 160 bar, and feed flow rate of 2.5 mL/min.

Table 4 – Factors and comparison between actual (Y) and predicted (FIT) responses.

Run order	Temperature (X_1)	Pressure (X_2)	Feed flow rate (X_3)	Responses Particle size (μm)	
				Y	FIT
1	60	160	2.5	90.930	88.855
2	60	140	2.5	37.670	37.780
3	40	150	1.0	24.580	23.025
4	40	140	2.5	28.620	30.695
5	50	160	4.0	54.640	55.160
6	50	150	2.5	37.670	37.670
7	40	160	2.5	33.910	33.800
8	40	150	4.0	26.490	26.080
9	50	150	2.5	37.670	37.670
10	60	150	1.0	54.640	55.050
11	50	160	1.0	54.640	56.305
12	50	140	1.0	26.490	25.970
13	50	140	4.0	32.980	31.315
14	50	150	2.5	37.670	37.670
15	60	150	4.0	54.640	56.195

A response surface regression analysis was carried out and the results of estimated regression coefficients of a second-order polynomial model for the optimization of experimental conditions aimed at particle size are shown in Table 5.

The mathematical model representing the encapsulation of fish oil within the range of studied variables was expressed by the following equation:

$$y = 2079.62 - 20.36X_1 - 22.69X_2 + 22.05X_3 + 0.04X_1^2 + 0.06X_2^2 - 0.71X_3^2 + 0.12X_1X_2 - 0.03X_1X_3 - 0.11X_2X_3 \quad (11)$$

where, X_1 = temperature, X_2 = pressure, and X_3 = feed flow rate.

The significant second-order polynomial equation at the 95% level of the optimization of experimental conditions of particle size is shown in Eq. (11). From Table 4, it was found that linear factors such as temperature (X_1) and pressure (X_2) showed negative coefficients whereas feed flow rate (X_3) showed positive coefficients. Negative values of the coefficient for the particle terms indicated that the particle size will decrease due to these particle terms. In contrast, positive values of coefficient indicated that the particle size will increase. Square factors for all three factors of temperature (X_1X_1), pressure (X_2X_2) showed positive coefficients whereas feed flow rate (X_3X_3) showed negative coefficients. The interaction or cross-product factors such as temperature and pressure (X_1X_2) also showed positive coefficients. Positive values of coefficient for the particle terms of temperature and pressure (X_1X_2) indicated that the particle size will increase due to these particle terms.

Moreover, the effect of experimental variables on the linear, quadratic, and interaction terms were tested by analysis of variance. The summary of the results obtained are shown in Table 6. By using lack-of-fit and coefficient determination (R^2), the suitability of the model can be revealed. The ratio of F at a probability (p) of 0.05 was used to assess the significance of the equation parameter for test variables.

3.2. Analysis of response surface methodology

The response optimizer was obtained and the results for the target goal at the optimum condition are shown in Figure 4.

Table 5 – Estimated regression coefficients of second-order polynomial model for optimization of encapsulation efficiency of fish oil powder.

Term	Coefficient	SE coefficient	T	p
Constant	2079.62	249.714	8.328	0.000
X_1	−20.36	1.830	−11.128	0.000
X_2	−22.69	3.159	−7.183	0.001
X_3	22.05	10.773	2.047	0.096
X_1X_1	0.04	0.010	3.859	0.012
X_2X_2	0.06	0.010	5.882	0.002
X_3X_3	−0.71	0.461	−1.531	0.186
X_1X_2	0.12	0.010	12.025	0.000
X_1X_3	−0.03	0.066	−0.479	0.652
X_2X_3	−0.11	0.066	−1.627	0.165

$R^2 = 99.53\%$ $R^2(\text{adj}) = 98.68\%$.
X_1 = temperature, X_2 = pressure and X_3 = feed flow rate.

Table 6 – Analysis of variance (ANOVA) for optimization of encapsulation efficiency of fish oil powder.

Source	DF	Seq SS	Adj SS	Adj MS	F	p	Status
Regression	9	4198.04	4198.04	466.448	117.24	0.000	Significant
Linear	3	3407.25	637.36	212.454	53.40	0.000	Significant
Square	3	204.07	204.07	68.022	17.10	0.005	Significant
Interaction	3	586.72	586.72	195.574	49.16	0.000	Significant
Residual error	5	19.89	19.89	3.979	—	—	—
Lack-of-fit	3	19.89	19.89	6.631	—	—	—
Pure error	2	0.00	0.00	0.000	—	—	—
Total	14	4217.93	—	—	—	—	—

Adj MS = adjusted mean square; Adj SS = adjusted sum of square; DF = degree of freedom; F = fischer; Seq SS = sequential sum of square.

The feasibility of the experiments for maximum goal was determined from the contour plot and the result is shown in Figure 5. Contour and surface plots for particle size at feasible optimum conditions are shown in Figures 5 and 6 with the temperature at 60°C, pressure at 150 bar, and feed flow rate at 1.36 mL/min.

In this study, results revealed that there was a significant interaction effect between temperature and pressure on the particle size. Furthermore, particle size increased with the increase of temperature and pressure. In order to have a better understanding of the significant effect ($p < 0.05$) of the statistical interaction of factors in response, a three dimensional surface and contour plot was recommended [30] for better understanding of the significant effect on the particle size and shown in Figures 5 and 6. The three dimensional surface plots showed the effects of particle size of fish oil powder at temperature of 60°C, pressure of 150 bar and feed flow rate of 1.36 mL/min. Each plot illustrated the particle size with one fixed value of variable.

3.3. *Optimization and model verification*

The suitability of the model for predicting the optimum response value was evaluated at the conditions of temperature at 60°C, pressure at 150 bar, and feed flow rate at 1.36 mL/min. Optimization using actual experimental values was tested using the t test (Minitab 16). It was found that there was no significant difference ($p > 0.05$) between predicted and verified values of the particle size. Thus, the model is significant and can be applied to estimate the optimization of particle size. Based on the optimum condition, four formulations were selected which was denoted as A series and other characterization parameters (moisture content, microencapsulation efficiency, *in vitro* release of oil through SIF and SGF and PV and surface morphology of powder).

3.4. *Characterization of fish oil emulsion*

Mean oil droplet diameters for all the formulations were found to be statistically significant ($p < 0.05$). In our study, emulsion droplet size varied from 3.75 μm to 13.7 μm. Emulsion containing low amounts of HPMC produced the smallest oil droplets with a mean diameter of < 4 μm. The mean diameter of the oil droplet of fish oil emulsion increased significantly with the total solid content. AF4 containing a low content of HPMC 15 cP, produced the largest droplet size of 13.7 μm, whereas AF1, containing a high amount of HPMC 15 cP, produced the smallest particle size of 3.75 μm. The use of fish oil in this study induced the increase of emulsion viscosity which is an important factor affecting the mean particle size. Jumaa and Müller [31] showed the dominating influence of the nature of the oil phase as well as the importance of the homogenizing conditions on processing and stability. They highlighted correlation between decrease of emulsion viscosity and mean size reduction. Moreover, emulsion droplets may coalesce during the intense shearing in the atomization

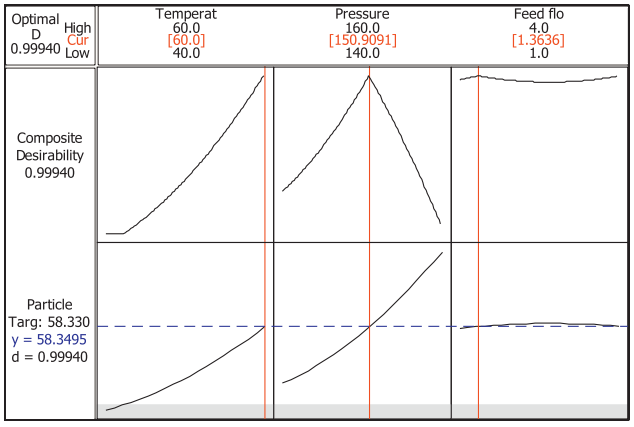

Figure 4 – Response optimizer at the optimum condition for target goal.

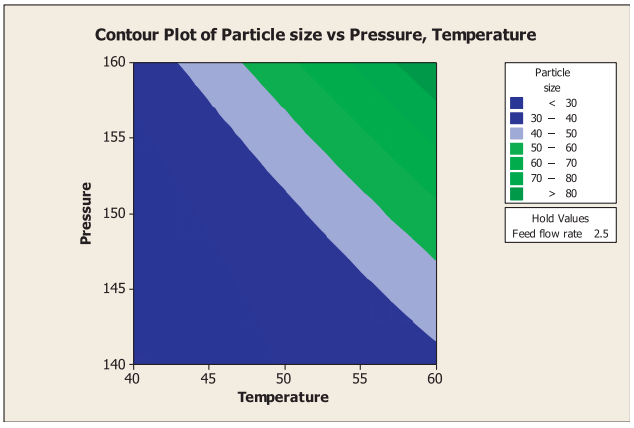

Figure 5 – Response contour plot of particle size (μm) at a feasible optimum condition.

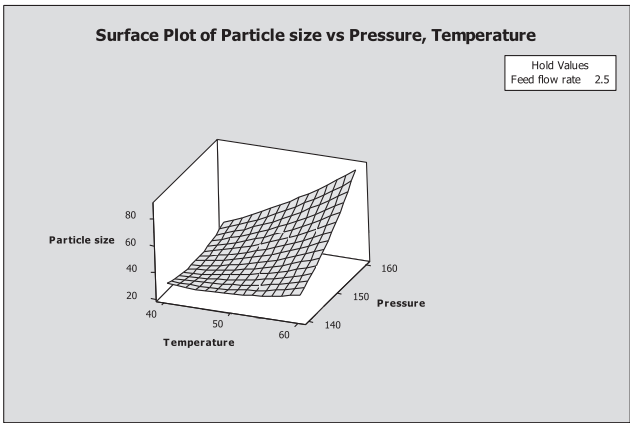

Figure 6 – Response surface plot of particle size (μm) at a feasible optimum condition.

device of the spray-dryer, resulting in larger droplet size distribution; this has been observed by several authors [32–34].

HPMC is itself a very viscous carrier material. As total solid content increased, emulsion viscosity also increased, which was expected, since a higher content of HPMC made the formulations more viscous. Higher viscosities prevent droplet flocculation and coalescence by slowing oil droplet movement [35]. Among all the formulations, AF1 showed a high viscosity of 63.27 mPa.s, whereas, AF4 showed a low viscosity of 11.83 mPa.s. High viscosity in the initial emulsion increased volatiles retention due to reduced droplets movement, favoring a rapid matrix formation and limiting the oil diffusion through the wall material [36]. Moreover, the different content and ratios of HPMC on the viscosity affects the formulations significantly ($p < 0.05$).

3.5. *Characterization of fish oil powder*

3.5.1. *Moisture content*

The moisture content of the powder is mainly caused by the relative humidity of the air in the dryer chamber. High moisture content may lead to caking/agglomeration of particles, promote microbial growth, and have negative effects on lipid stability since this factor has been reported as being very important [37]. Moisture content of the fish oil powders obtained from the supercritical antisolvent process is shown in Table 8. The moisture content of the fish oil powder was in the range from 3.56% to 4.91%. Supercritical antisolvent conditions possessed the greatest effect on the moisture content. The maximum moisture specification for most dried powders in the food industry is between 3% and 4% [38,39].

In this study, AF2 showed less moisture content of 3.56% and AF4 showed higher moisture content of 4.91% and moreover, all the moisture content of different formulations were compared and found statistically significant ($p < 0.05$).

3.5.2. *Microencapsulation efficiency*

Encapsulation efficiency is an important parameter for evaluating performance of materials as encapsulation agents. Furthermore, for ingredients susceptible to oxidation, the portion of core material that remains on the surface is particularly important – materials on the surface are believed to be more susceptible to oxidation as they do not have the benefit of a carbohydrate barrier film. Particle flow and wetting characteristics also are impacted by surface fat content [40]. Encapsulation efficiency was calculated based on total oil content and surface oil content. Encapsulation efficiency of the encapsulated powders varied from 69.55% to 81.75% and was significantly influenced ($p < 0.05$) by the polymer compositions. As the HPMC content increased, the encapsulation efficiency of fish oil also increased (Figure 7). During the experiments, the temperature and pressure were kept at 60°C and 150 bar, respectively, which increased the drying rate of the droplets causing the formation of crust on the particle surface. This crust provided a solid membrane around the particles preventing the leaching of oil from the droplets. Encapsulation efficiency was higher for particles produced from emulsions with higher solid content, i.e., encapsulation efficiency of AF1 was high among all the formulations.

The influence of oil concentration on the encapsulation efficiency can also be related to the emulsion viscosity. As stated before, lower oil content resulted in higher emulsion viscosity (for the same solid content), which makes it difficult for the oil to diffuse to the drying particle surface. Similar results were obtained by Tan et al [41] in the microencapsulation of fish oil by spray drying, using modified starch as wall material. The authors found that higher oil:wall material ratio (1.5:1) resulted in lower encapsulation efficiency (47.8%), compared to an oil:wall material ratio of 1:1, which led to an encapsulation efficiency of 68.6%. McNamee et al [42], when encapsulating soy oil with gum Arabic, observed that the encapsulation efficiency decreased from 100% to 48% when the oil:gum ratio increased from 0.25 to 5.0. With respect to total solid content, this variable had a positive effect on the encapsulation efficiency, i.e., higher solid content resulted in higher encapsulation efficiency. This result can be attributed to the emulsion droplet size, which decreased when total solid content increased. Frascareli et al. [43] studied the encapsulation of coffee oil where the authors found that the encapsulation efficiency (48–82 %) was significantly influenced by the total solid content.

3.5.3. In vitro *determination of encapsulated oil after exposure to SGF and SIF*

The influence of the wall component on the microcapsules digestibility was assessed by means of *in vitro* gastric and

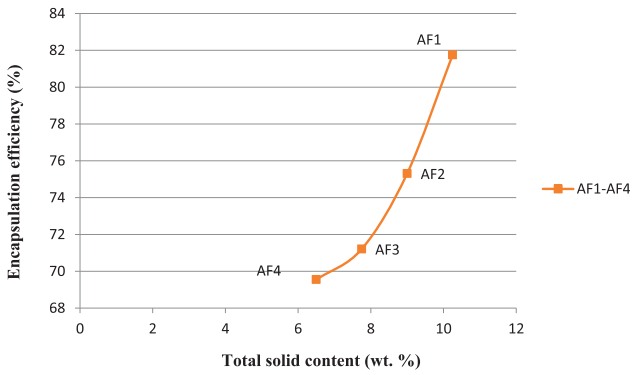

Figure 7 – Effect of total solid content on encapsulation efficiency.

intestinal digestion. The amount of oil obtained after the *in vitro* digestion, expressed as % recovered oil after *in vitro* digestion, has been evaluated considering the different types of microcapsule wall components. Besides, with the aim to address that the encapsulated oil was released from the capsules due to the action of the digestion process rather than the solubility of the wall components in the aqueous media, the microcapsule powders were submitted to the same digestive procedure using purified water instead of SGF and SIF.

In this study, *in vitro* gastric and intestinal digestion of the encapsulated oil was significantly influenced by the composition of wall material ($p < 0.05$). The percentage of oil released after SGF treatment was in the range of 18.35–45.69% (Table 8). Formulation AF1 released the lowest amount of oil (18.35%) and AF4 released the highest amount of oil (45.69%) among all the formulations. The percentage of oil release after the exposure to SGF and SIF was found to be higher than the SGF alone (Table 7). Formulation AF1 released the least percentage of oil (28.99%), whereas AF4 released a high percentage of oil (74.98%). Patten et al. [23] found that digestion in SGF and intestinal fluid demonstrated that only 4–6% of oil was released from the dried emulsion formulations.

3.5.4. *Particle surface morphology*

The structures of microcapsules observed by FESEM are presented in Figure 8 with magnification of 2000×. In all the samples, the diameter was 10 μm. The FESEM image showed that particles formed spherical structures with no internal void. The diameters of microcapsules are probably dependent on the type and concentration of wall materials, parameters of homogenization. Figure 8 showed that there were some partly damaged capsules and formation of the wrinkled surface of the encapsulated oil was also observed in some areas of the particles.

Formulations containing higher concentration of HPMC 15 cP tended to have higher viscosity (63.27 mPa.s) than other formulations, hence restraining the elasticity of the droplet during drying. Moreover, AF1 containing high concentration of HPMC 15 cP, seemed to have less wrinkled surface than the ones at lower concentration of HPMC 15 cP. For instance, the viscosity of the formulations increased from 11.83 mPa.s to 63.27 mPa.s, whereas the solid content also increased from 6.5% to 10.25%. Bubble inflation can be rampant at lower concentrations of HPMC 15 cP, which caused formation of more dented surface in the final stage of the drying process. Moreover, there were no cracks or holes observed on the surface of any of the formulations. Regardless of their morphology, the particle surface irregularity did not cast much effect on the characterization parameters of the encapsulated fish oil. Moreover, our observations match those made by Kolanowski et al. [15] and Wu and Xiao [17].

Table 7 – Viscosity and droplet size of emulsions with different solid content.

Formulations	Total solid content (wt. %)	Viscosity (mPa. s)	Droplet size, $D_{4,3}$ (μm)
AF1	10.25	63.27 ± 0.15^{a}	3.75 ± 0.04^{a}
AF2	9.0	42.90 ± 0.10^{b}	7.24 ± 0.05^{b}
AF3	7.75	29.30 ± 0.10^{c}	12.77 ± 0.06^{c}
AF4	6.5	11.83 ± 0.06^{d}	13.7 ± 0.06^{d}

Values are average of triplicate ($n = 3$) analyses ± standard deviation.
[a, b, c, d] Different letters within each column are significantly different at $p < 0.05$ when compared to AF1 with AF2, AF3 and AF4 values using Tukey's HSD *post hoc* test.

3.5.5. *Bulk density and tapped density of powder*

Particles with bulk and tapped densities were strongly influenced by the wall material ratio and composition. In addition, higher densities were observed with a higher presence of HPMC. Because of the smaller molecules of HPMC, there is a greater possibility of wall material accommodation into the open spaces between molecules, which permits the formation of more compact structures with higher densities. In this study, the bulk density was in a range of 0.141–0.221 g mL^{-1} (Table 9) and the value of tapped density was in the range 0.166–0.260 g mL^{-1} (Table 9). Densities varying from 0.52 g mL^{-1} to 0.67 g mL^{-1} were found for the encapsulation of pigments [44]. The higher values observed in the investigation of Cai and Corke [44] compared to the present work, may be related to the application of only maltodextrin as a wall material, which provides a reduced molecular structure and produces more compact particles. Finney et al [37] studied the encapsulation of orange essential oil where the authors found high tapped density from 0.48 g $mL^{-1}$to 0.65 g mL^{-1}.

3.5.6. *Flowability and cohesiveness of the powder*

Powder flowability is usually applied as a quality parameter for the dried microcapsules. In general, CI and HR are used to assess powder flowability [45]. In this study, CI value varied from 10.90% to 15.06% (Table 9). The results showed that the powders prepared by the supercritical antisolvent process had good flow characteristics (Table 3). Quispe-Condori et al [46] studied the encapsulation of flax oil where the authors found the CI very high. So, the flowing property was poor. Similar results were obtained by Xue et al [47], where the authors found that the flowing property of the powders was poor. The higher HR indicated that the powder was more cohesive and less able to flow freely. In this study, HR was in a range from 1.13 to 1.18 which showed that the powder has a good flow property. Moreover, the Tukey test showed no real change in the powder flowability ($p > 0.05$).

3.5.7. *Particle density*

Particle density was influenced by the ratio and concentration of the wall material and rate of feed emulsion (nature of the encapsulate and solid contents). In this study, the particle density ranged from 0.833 g mL^{-1} to 0.950 g mL^{-1} (Table 9). Botrel et al [48] studied the encapsulation of oregano essential oil where they found the particle density in the range from 0.74 g mL^{-1} to 0.92 g mL^{-1}. Abadio et al [49] found that with the increase in the concentration of encapsulating material, there was a decrease in the true density of the microcapsules of pineapple juice, probably due to the lower moisture content. Particle density can also decrease due to steam formation in the drying droplet causing the expansion of the particle the

Table 8 – Characteristics of encapsulated powder of different formulations.

Formulation	Moisture (wt. %)	Microencapsulation efficiency (%)	Oil release (%)	
			SGF digestion	SGF and SIF digestion
AF1	3.6 ± 0.06^{a}	81.75 ± 0.15^{a}	18.35 ± 0.97^{a}	28.99 ± 0.67^{a}
AF2	3.56 ± 0.03^{a}	75.31 ± 0.15^{b}	28.33 ± 0.63^{b}	40.63 ± 0.78^{b}
AF3	4.43 ± 0.07^{b}	71.21 ± 1.23^{c}	37.54 ± 0.79^{c}	54.49 ± 1.41^{c}
AF4	4.91 ± 0.07^{c}	69.55 ± 1.55^{d}	45.69 ± 0.58^{d}	74.98 ± 1.71^{d}

Values are average of triplicate ($n = 3$) analyses ± standard deviation.
SGF = simulated gastric fluid; SIF = simulated intestinal fluid.
[a, b, c, d] Different letters within each column are significantly different at $p < 0.05$ when compared to AF1 with AF2, AF3 and AF4 values using Tukey's HSD *post hoc* test.

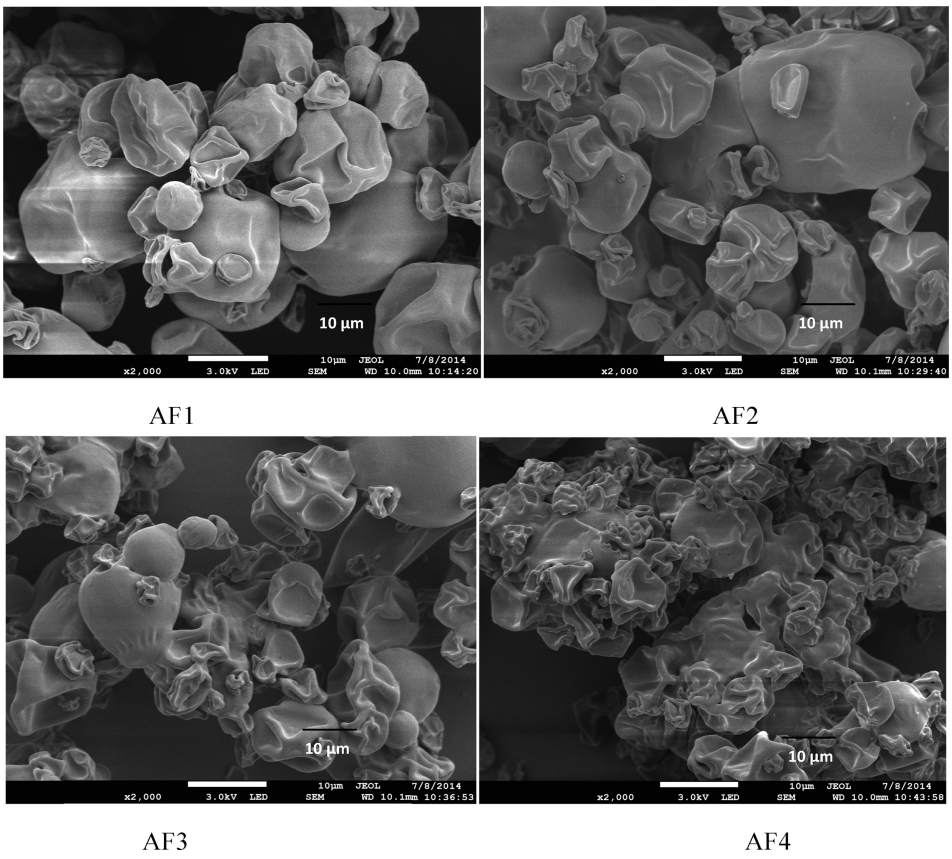

Figure 8 – Morphology of fish oil powder (AF1, AF2, AF3, and AF4) at different concentration.

Table 9 – Characteristics of encapsulated powder of different formulations.

Formulation	Bulk density ($g\ mL^{-1}$)	Tapped density ($g\ mL^{-1}$)	Flowability & cohesiveness		Particle density ($g\ mL^{-1}$)
			Carr index (%)	Hausner ratio	
AF1	0.221 ± 0.002^{a}	0.260 ± 0.002^{a}	10.90 ± 1.23^{a}	1.18 ± 0.02^{a}	0.833 ± 0.006^{a}
AF2	0.191 ± 0.003^{b}	0.217 ± 0.004^{b}	11.84 ± 0.77^{a}	1.13 ± 0.01^{a}	0.873 ± 0.012^{a}
AF3	0.164 ± 0.003^{c}	0.193 ± 0.001^{c}	15.05 ± 1.41^{a}	1.18 ± 0.02^{a}	0.917 ± 0.006^{a}
AF4	0.141 ± 0.002^{d}	0.166 ± 0.002^{d}	15.06 ± 0.62^{a}	1.18 ± 0.01^{a}	0.950 ± 0.010^{b}

Values are average of triplicate ($n = 3$) analyses ± standard deviation.
[a, b, c, d] Different letters within each column are significantly different at $p < 0.05$ when compared to AF1 with AF2, AF3 and AF4 values using Tukey's HSD *post hoc* test.

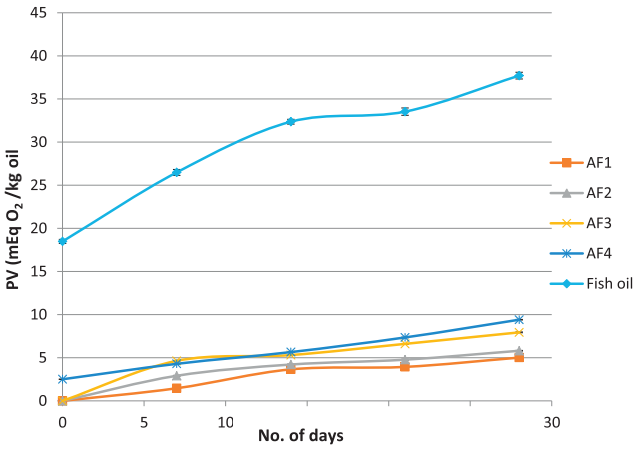

Figure 9 – Effect of storage time on the peroxide value of formulation AF1, AF2, AF3, AF4.

dimensions of which become fixed even with the continuity of the drying process [37].

3.5.8. *PV of the powder*

In our study, PV of all the formulations produced by supercritical antisolvent process was found to be lower compared to previous studies. Young et al [50] reported that PV of crude fish oil was 3–20 mEq/kg oil. The values obtained for produced microparticles in this research were well below the acceptable limit of 20 mEq O_2/kg oil. Initially, PV of AF4 was 2.51 mEq O_2/kg oil which increased to 9.41 mEq O_2/kg oil in 28 days, whereas, formulation AF2 and AF3 increased to 5.81 mEq O_2/kg oil and 7.94 mEq O_2/kg oil, respectively in 28 days (Figure 9). Among all the formulations, AF1 containing higher concentration of higher content of HPMC 15 cP possessed lower PV, i.e., 5.02 mEq O_2/kg oil in 28 days.

It is argued that the early formation of particle crust and higher encapsulation efficiency was mainly responsible for this lower PV, i.e., it shielded the oil from oxidation attacks. According to Tonon et al [51], the lower the encapsulation efficiency, the higher was the amount of oil present in the particle surface. This unencapsulated oil was more rapidly oxidized than its encapsulated counterpart due to the direct contact with the oxygen of drying air. Kolanowski et al [15] studied the encapsulation of fish oil with modified cellulose and found that the microencapsulated fish oil showed acceptable oxidative stability compared to bulk fish oil. In another study conducted by Pourashouri et al [52] on the encapsulation of fish oil, the encapsulated oil was found to be more stable than the nonencapsulated oil. Because of the ballooning and expansion, the wall materials become too fragile which results in a reasonably high amount of PV of the encapsulated oil. Ghorbanzade et al [53] studied the nanoencapsulation of fish oil using nano-liposome as an encapsulant. The authors observed that there was a significant reduction in acidity, syneresis and PV of encapsulated fish oil which is more stable than the nonencapsulated fish oil. The results of gas chromatography analyses revealed that after 21 days storage, yogurt fortified with nanoencapsulated fish oil had higher DHA and EPA contents than yogurt containing free fish oil.

4. Conclusion

From our study, it was proved that HPMC was found to be an effective carrier material for the successful encapsulation of fish oil. Overall, the results showed that every selected response has been influenced significantly by the different ratios and concentrations of wall materials. Higher solid concentration led to bigger particle size, lower moisture content, and fewer dented surfaces, which improved particle flowability. Moreover, microencapsulation using the higher concentration of HPMC improved the particle density, wettability, and porosity of the powder particles compared to the lower concentration of HPMC. Formulation AF1 provided the highest encapsulation efficiency and stability against oxidation among all other formulations produced by spray drying. Moreover, due to easy availability of this polymer, HPMC, and the findings of this research, the formulation and encapsulation of any pharmaceutical or nutraceutical grade oil can be encapsulated with the supercritical antisolvent technique for their industrial application.

Conflict of interest

All contributing authors declare no conflict of interest.

Acknowledgments

The work was funded by the exploratory research grant scheme, number ERGS13-028-0061 of the Ministry of Higher Education, Malaysia. The authors extend their appreciation to the International Scientific Partnership Program ISPP at King Saud University, Riyadh, Saudi Arabia, for funding this research work through ISPP# 0026. The authors would also like to thank to Mr Mahbubul Karim of Incepta Pharmaceuticals Ltd, Bangladesh for providing us the polymers (HPMC 15 cP and HPMC 5 cP).

REFERENCES

[1] Stone NJ. Fish consumption, fish oil, lipids, and coronary heart disease. Am J Clin Nutr 1997;65:1083–6.
[2] Salem N, Simopoulos AP, Galli C, Lagarde M, Knapp H. Proc. 2nd Congr ISSFAL on fatty acids and lipids from cell biology to human disease. Lipids 1998;31(Suppl. 1):11–32.
[3] Simopoulos AP, Leaf A, Salem Jr N. Essentiality of and recommended dietary intakes for omega-6 andomega-3 fatty acids. Ann Nutr Metab 1999;43:127–30.
[4] Champagne CP, Fustier P. Microencapsulation for the improved delivery of bioactive compounds into foods. Curr Op Biotech 2007;18:184–90.
[5] Fahim TK, Zaidul ISM, Abu Bakar MR, Salim UM, Awang MB, Sahena F, Jalal KCA, Sharif KM, Sohrab MH. Particle formation and micronization using non-conventional techniques-review. Chem Eng Process: Process Intensification 2014;86:47–52.
[6] Sanguansri L, Augustin MA. Microencapsulation and delivery of omega-3 fatty acids. Func Food Ingred Nutra, Proc Technol 2016:373–408.

[7] Augustin MA, Sanguansri L. Encapsulation of bioactives. In: Food materials science. New York: Springer; 2008. p. 577–601.
[8] Jimenez M, Garcia HS, Beristain CI. Spray-drying microencapsulation and oxidative stability of conjugated linoleic acid. Eur Food Res Technol 2004;219:588–92.
[9] Drusch S, Serfert Y, Van Den Heuvel A, Schwarz K. Physicochemical characterization and oxidative stability of fish oil encapsulated in an amorphous matrix containing trehalose. Food Res Int 2006;39:807–15.
[10] Velasco J, Marmesat S, Dobarganes C, Márquez-Ruiz G. Heterogeneous aspects of lipid oxidation in dried microencapsulated oils. J Agr Food Chem 2006;54:1722–9.
[11] Drusch S, Mannino S. Patent-based review on industrial approaches for the microencapsulation of oils rich in polyunsaturated fatty acids. Trends Food Sci Technol 2009;20:237–44.
[12] Mehrad B, Shabanpour B, Jafari SM, Pourashouri P. Characterization of dried fish oil from Menhaden encapsulated by spray drying. AACL Bioflux 2015;8:57–69.
[13] Pourashouri P, Shabanpour B, Razavi SH, Jafari SM, Shabani A, Aubourg SP. Impact of wall materials on physicochemical properties of microencapsulated fish oil by spray drying. Food Bioproc Tech 2014;7:2354–65.
[14] Klaypradit W, Huang YW. Fish oil encapsulation with chitosan using ultrasonic atomizer. LWT – Food Sci Technol 2008;41:1133–9.
[15] Kolanowski W, Laufenberg G, Kunz B. Fish oil stabilisation by microencapsulation with modified cellulose. Int J Food Sci Nutr 2004;55:333–43.
[16] Christensen KL, Pedersen GP, Kristensen HG. Preparation of redispersible dry emulsions by spray drying. Int J Pharm 2001;212:187–94.
[17] Wu KG, Xiao Q. Microencapsulation of fish oil by simple coacervation of hydroxypropyl methylcellulose. Chin J Chem 2005;23:1569–72.
[18] Karim FT, Sarker ZM, Ghafoor K, Al-Juhaimi FY, Jalil RU, Awang MB, Amid M, Hossain MD, Khalil HP. Microencapsulation of fish oil using hydroxypropyl methylcellulose as a carrier material by spray drying. J Food Process Preserv 2015;40:140–53.
[19] Chong GH, Yunus R, Abdullah N, Choong TS, Spootar S. Coating and encapsulation of nanoparticles using supercritical antisolvent. Am J Appl Sci 2009;6:1352–8.
[20] Anwar SH, Kunz B. The influence of drying methods on the stabilization of fish oil microcapsules: comparison of spray granulation, spray drying, and freeze drying. J Food Eng 2011;105:367–78.
[21] García E, Gutiérrez S, Nolasco H, Carreón L, Arjona O. Lipid composition of shark liver oil: effects of emulsifying and microencapsulation processes. Eur Food Res Technol 2006;222:697–701.
[22] Chung C, Sanguansri L, Augustin MA. In vitro lipolysis of fish oil microcapsules containing protein and resistant starch. Food Chem 2011;124:1480–9.
[23] Patten GS, Augustin MA, Sanguansri L, Head RJ, Abeywardena MY. Site specific delivery of microencapsulated fish oil to the gastrointestinal tract of the rat. Dig Dis Sci 2009;54:511–21.
[24] Pharmacopeia US. National Formulatory. Rockville, MD: USP 24 NF 19; 2000.
[25] Goula AM, Adamopoulos KG. Effect of maltodextrin addition during spray drying of tomato pulp in dehumidified air: II. Powder properties. Drying Technol 2008;26:726–37.
[26] Carr RL. Evaluating flow properties of solids. Chem Eng 1965;72:163–8.
[27] Hausner HH. Friction conditions in a mass of metal powder. Int J Powd Met 1967;3:7–13.
[28] A/S Niro Atomizer, Copenhagen, Denmark. Determination of particle density, content of occluded air and interstitial air. In: Sørensen IH, Krag J, Pisecky J, Westergaard V, editors. Analytical methods for dry milk products. 4th ed. Copenhagen: De Forenede Trykkerier A/S; 1978c. p. 52–3.
[29] [AOCS] American Oil Chemists' Society. Official methods and recommended practices of the American Oil Chemists' Society 2009; Method Cd 8–53. Champaign, IL: AOCS Press.
[30] Farhadian A, Jinap S, Faridah A, Zaidul IS. Effects of marinating on the formation of polycyclic aromatic hydrocarbons (benzo [a] pyrene, benzo [b] fluoranthene and fluoranthene) in grilled beef meat. Food Control 2012;28:420–5.
[31] Jumaa M, Müller BW. The effect of oil components and homogenization conditions on the physicochemical properties and stability of parenteral fat emulsions. Int J Pharm 1998;163:81–9.
[32] Keogh MK, O'Kennedy BT. Milk fat microencapsulation using whey proteins. Int Dairy J 1999;9:657–63.
[33] Pedersen GP, Fäldt P, Bergenståhl B, Kristensen HG. Solid state characterisation of a dry emulsion: a potential drug delivery system. Int J Pharm 1998;171:257–70.
[34] Millqvist-Fureby A. Characterisation of spray-dried emulsions with mixed fat phases. Coll Surf B: Bioint 2003;31:65–79.
[35] Tsaliki E, Pegiadou S, Doxastakis G. Evaluation of the emulsifying properties of cottonseed protein isolates. F Hydr 2004;18:631–7.
[36] Sheu TY, Rosenberg M. Microstructure of microcapsules consisting of whey proteins and carbohydrates. J Food Sci 1998;63:491–4.
[37] Finney J, Buffo R, Reineccius GA. Effects of type of atomization and processing temperatures on the physical properties and stability of spray-dried flavors. J Food Sci 2002;67:1108–14.
[38] Serfert Y, Drusch S, Schwarz K. Chemical stabilisation of oils rich in long-chain polyunsaturated fatty acids during homogenisation, microencapsulation and storage. Food Chem 2009;113:1106–12.
[39] Drusch S. Sugar beet pectin: a novel emulsifying wall component for microencapsulation of lipophilic food ingredients by spray-drying. Food Hydrcoll 2007;21:1223–8.
[40] Drusch S, Berg S. Extractable oil in microcapsules prepared by spray-drying: localisation, determination and impact on oxidative stability. Food Chem 2008;109:17–24.
[41] Tan LH, Chan LW, Heng PW. Effect of oil loading on microspheres produced by spray drying. J Microencapsul 2005;22:253–9.
[42] McNamee BF, O'Riorda ED, O'Sullivan M. Emulsification and microencapsulation properties of gum arabic. J Agri Food Chem 1998;46:4551–5.
[43] Frascareli EC, Silva VM, Tonon RV, Hubinger MD. Effect of process conditions on the microencapsulation of coffee oil by spray drying. Food Bio Process 2012;90:413–24.
[44] Cai YZ, Corke H. Production and properties of spray-dried Amaranthus betacyanin pigments. J Food Sci 2000;65:1248–52.
[45] Fitzpatrick JJ, Iqbal T, Delaney C, Twomey T, Keogh MK. Effect of powder properties and storage conditions on the flowability of milk powders with different fat contents. J Food Eng 2004;64:435–44.
[46] Quispe-Condori S, Saldaña MD, Temelli F. Microencapsulation of flax oil with zein using spray and freeze drying. LWT – Food Sci Technol 2011;44:1880–7.
[47] Xue F, Li C, Liu Y, Zhu X, Pan S, Wang L. Encapsulation of tomato oleoresin with zein prepared from corn gluten meal. J Food Eng 2013;119:439–45.

[48] Alvarenga Botrel D, Vilela Borges S, Victória de Barros Fernandes R, Dantas Viana A, Maria Gomes da Costa J, Reginaldo Marques G. Evaluation of spray drying conditions on properties of microencapsulated oregano essential oil. Int J Food SciTech 2012;47:2289–96.
[49] Abadio FD, Domingues AM, Borges SV, Oliveira VM. Physical properties of powdered pineapple (Ananas comosus) juice––effect of malt dextrin concentration and atomization speed. J Food Eng 2004;64:285–7.
[50] Young SL, Sarda X, Rosenberg M. Microencapsulating properties of whey proteins. 2. Combination of whey proteins with carbohydrates. J Dairy Sci 1993;76:2878–85.
[51] Tonon RV, Grosso CR, Hubinger MD. Influence of emulsion composition and inlet air temperature on the microencapsulation of flaxseed oil by spray drying. Food Res Int 2011;44:282–9.
[52] Pourashouri P, Shabanpour B, Razavi SH, Jafari SM, Shabani A, Aubourg SP. Oxidative stability of spray-dried microencapsulated fish oils with different wall materials. J Aquatic Food Prod Technol 2014;23:567–78.
[53] Ghorbanzade T, Jafari SM, Akhavan S, Hadavi R. Nano-encapsulation of fish oil in nano-liposomes and its application in fortification of yogurt. J Food Chem 2017;216:146–52.